Available online at www.sciencedirect.com
ScienceDirect
ELSEVIER
Nuclear Instruments and Methods in Physics Research A 576 (2007) 52–55
NUCLEAR INSTRUMENTS & METHODS IN PHYSICS RESEARCH Section A
www.elsevier.com/locate/nima

Development of a high-efficiency high-resolution imaging detector for 30–80 keV X-rays

U.L. Olsen[a,*], X. Badel[b], J. Linnros[b], M. Di Michiel[c], T. Martin[c], S. Schmidt[a], H.F. Poulsen[a]

[a]*Centre for Fundamental Research: Metal Structures in Four Dimensions, Risø National Laboratory, 4000 Roskilde, Denmark*
[b]*IMIT, Royal Institute of Technology, Electrum 229, 164 40 Kista, Sweden*
[c]*ESRF, 6 rue Jules Horowitz, 38043 Grenoble Cedex, France*

Available online 6 February 2007

Abstract

A newly developed fabrication method makes the formation of deep structured scintillator screens possible. We demonstrate that electrochemical etching in silicon can be used to produce regular arrays of 120 μm deep pores with a 4 μm pitch. A layer of SiO_2 is grown on the pore walls and CsI:Tl is melted into the pores, resulting in a structure with a high refractive index core surrounded by a quartz cladding, providing efficient light guiding. The efficiency and radiation hardness of the scintillator is evaluated in realistic environment at beamline ID15 at the ESRF synchrotron. The efficiency is measured to be a factor two higher than a planar YAG: Ce scintillator of equal thickness, while radiation damage is found to be neglectable for doses up to at least 2×10^4 Gy.
© 2007 Elsevier B.V. All rights reserved.

PACS: 07.85.Fv; 82.47.Wx; 61.80.−x

Keywords: 3DXRD; Scintillators; CsI:Tl; Electrochemical etching; Efficiency; Radiation damage

1. Introduction

In materials science X-rays are used for non-destructive probing of bulk properties. As the community gains access to synchrotron radiation they are progressing to harder X-rays to better investigate larger bulk samples; at the same time the need to resolve details at a micron level continuously increases, bringing forth the need for high-resolution X-ray detection at energies between 30 and 80 keV.

Presently, for such purposes detectors comprising a scintillator optically linked to a charged-coupled device (CCD) [1] are used almost universally. Unfortunately, this design has two serious drawbacks. Firstly, the visible photons are emitted in a Lambert like distribution within the scintillator, and hence the spatial resolution of the detector is limited by the thickness of the scintillating screen. Secondly, for support purposes, scintillators are typically mounted on thicker substrates, and Compton scattering and fluorescence in the substrates gives rise to considerable tails in the line spread function (LSF).

As an example, a typical scintillator used at the European Synchrotron Radiation Facility (ESRF) is a 6-μm-thick crystal of YAG, LAG, or YAP doped with Cerium on a 100-μm-thick substrate. This is used in hard X-ray tomographic experiments with a resolution of 2 μm [2,3], but in the white beam used for this work the efficiency is only approximately 1.1%.

The strong coupling between spatial resolution and efficiency reduces options for time-resolved studies. This is true for tomographic studies, but the problem has been accentuated by the recent introduction of 3DXRD microscopy [4].

These disadvantages are well known and several solutions have been suggested in the literature. One direction of research is towards semiconductor detectors with 3D anodes [5]. A second direction of research is towards manufacturing of scintillation screens confining and guiding the secondary emitted photons through the screen [6,7].

In this paper, we present the design and test of a first generation structured scintillator for a high-efficiency,

*Corresponding author. Tel.: +45 4677 5842; fax: +45 4677 5758.
E-mail address: ulrik.lund.olsen@risoe.dk (U.L. Olsen).

0168-9002/$ - see front matter © 2007 Elsevier B.V. All rights reserved.
doi:10.1016/j.nima.2007.01.119

high-resolution detector to work in the range above 30 keV using an alternative for producing light guiding screens by means of electrochemical etching [8,9]. For this initial work a pore pitch of 4 μm was chosen.

2. Design

The scintillator presented here is an adaptation of a design used by Badel [8]. An array of pores is etched into a silicon wafer, which is opaque to visible light. A thin surface layer of silicon dioxide on the porewalls acts as waveguide cladding with a refractive index of 1.45. The pores are filled with the scintillating material CsI and its refractive index of 1.73 gives the pores internal reflection at angles above 56° from normal incidence. Assuming a Lambert-like emission of visible photons, 8.5% of the emitted photons will reach the pore end.

For the presented samples pores are electrochemically etched in silicon in a square pattern with a 4 μm pitch. The pores are 3.1 μm wide square cylinders 65–125 μm deep, and the pore wall surface is a 250 nm layer of silicon dioxide. The pore filling is CsI doped with 0.1% per weight thallium. The design gives a ratio of the active area of 0.4 making the total absorption 16% with 50 keV X-rays.

3. Fabrication

Fabrication involves three steps. The first step takes place in clean room environment and produces an array of pits in the silicon. The second step is the electrochemical etching process [10]. The third step is filling of the pores with scintillating material by melting CsI:Tl powder. This process was hardly explored prior to this study and is here merely developed to working order but not optimized for maximum performance.

3.1. Cleanroom process

The scintillating screen is made on 500-μm-thick silicon N-type wafers doped with phosphor; the resistivity is 20–40 Ω cm. The pattern of the pore array is defined using standard lithography techniques with an XLS-stepper. The developed wafers are reactive ion etched (RIE) to open the oxide and the resist is then removed. In a KOH etch, inverted pyramids are formed in the pattern determined by the oxide mask. These indents in the silicon are the starting points for the growth of the pores during the electrochemical etching step.

3.2. Etching

After the wafers exit the clean room, they are cut into chips with dimensions accepted in the etching chamber. The presented samples were etched for 8500 s in a 3.3 wt% solution of HF using a current density of 4.5 mA/mm^2 and a bias of 0.4 V.

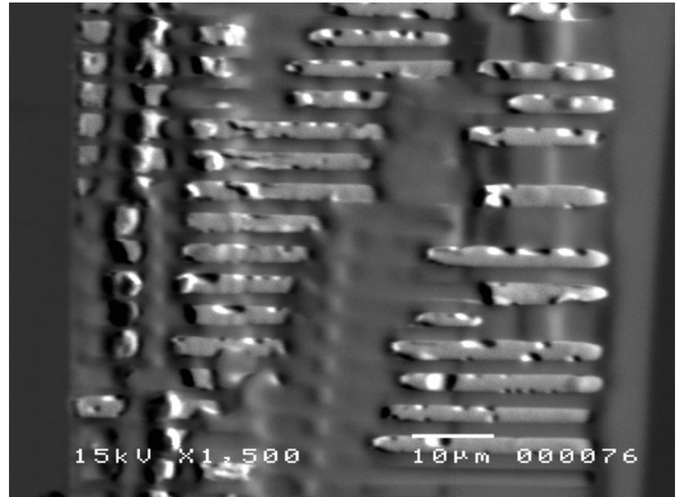

Fig. 1. SEM image of the bottom of filled pores, with the surface to the left. When the edge is exposed by cleaving, the soft CsI tends to crack and escape the pores.

The etched silicon array is subsequently thermally oxidized for 10 min at 1100 °C to grow 250 nm SiO_2. The SiO_2 is vital for the wave guiding ability but another significant effect is the increased wetting angle of CsI on SiO_2 compared to CsI on silicon. Tests we have performed show that CsI can penetrate pores even an order of magnitude thinner than the ones presented here.

3.3. Filling

CsI doped with 1000 ppm thallium in powder form is placed on top of the pores and placed in an oven with a pure nitrogen atmosphere (to reduce contamination during the filling process). The chip is heated to the melting temperature of CsI at 621 °C in approximately 10 min and kept at this temperature for 5 min to ensure a complete phase transformation. Subsequently, the chip is cooled down by free heat conduction reaching 100 °C in 1 h or using a controlled cooling of 5 K/min. The purpose of the differentiated cooling has been to investigate the role of the annealing on the thallium content, since it is expected that thallium evaporates from the CsI matrix during heating and that the time at elevated temperatures should be kept at a minimum.

Surface finishing consists of a coarse removal of CsI with a blade, followed by polishing with diamond lapping sheets. Four samples are spin coated with a 0.5 μm anti-reflecting surface layer of polyimide with refractive index 1.57 or poly methyl methacrylate (PMMA) with refractive index 1.44. The filled array is shown in Fig 1.

4. X-ray characterization

The parameters of the seven screens prepared for testing at the synchrotron at ESRF in Grenoble are presented in Table 1. The goal is an evaluation of the scaled down design and of exposing the screens to a realistic working

Table 1
Parameters for scintillators

Sample	Pore depth (μm)	Cooling (K/min)	Surface coating
23	70	5	—
24	70	5	Polyimide
25	70	Free cond.	PMMA
26	70	Free cond.	—
27	125	5	Polyimide
28	60	5	PMMA
29	65	5	—

environment. One of the most significant questions for this test is the performance of the screen after subjection to the intense radiation produced by the synchrotron. The function of the narrow pores as waveguides represents another unknown but vital parameter. The main test goals are hence an estimate of the efficiency and a measure of the radiation hardness.

At the experimental hutch of ID15 the monochromatic beam is supplied via two Laue crystals with approx. 100 eV bandwidth at 50 keV, this is ideally suited to expose the samples to a high amount of radiation at a specific energy.

The setup is composed of the incoming beam defined by horizontal and vertical slits detected by a sample scintillator mounted in front of a reflective lens and via an X-ray transparent mirror reflected on a CCD.

4.1. Efficiency

Efficiency measurements are obtained from flood field images, from which the intensity threshold of the 0.2% lightest pixels is found. Each sample is measured in different areas and the intensity in each image is calibrated with a simultaneous measurement from a silicon diode with approx. 8% absorption at 50 keV.

The intensity is compared to a well-characterized free-standing 100 μm YAG: Ce reference and is seen in Fig. 2 to be doubled for some of the structured samples confirming the potential of the design for high efficiency.

This first batch of scintillators has a very high degree of inhomogenity, which so far is attributed to surface effects like polishing. Coating the sample surface with a polymer enhanced the emission, and particularly a PMMA coating produced the greatest effect.

4.2. Radiation damage

To evaluate the radiation hardness, a specific part of a sample was selected and the efficiency was monitored at intervals during continuous exposure to the beam. The efficiency was again calibrated according to the intensity of the incoming X-ray beam and the normalized intensity is seen from the graph in Fig. 3 and shows no clear decreasing trend. The intensity is within 2% of the initial value even

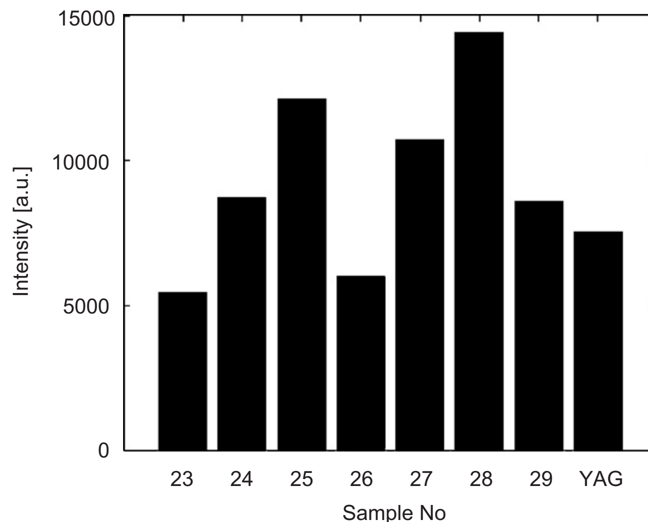

Fig. 2. Image intensities obtained with selected samples. Generally samples with a PMMA coating give a higher intensity. Also shown is the intensity of a comparable YAG scintillator.

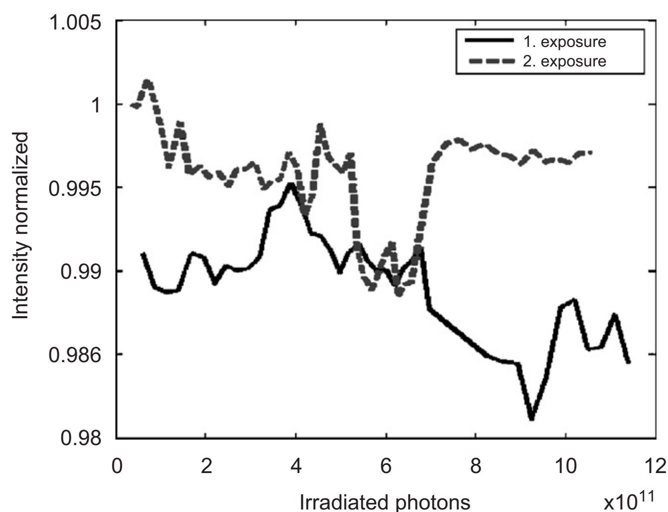

Fig. 3. Graph showing average image intensity after prolonged exposure to the direct synchrotron beam. The two curves are obtained for different areas of the same sample.

after a dose of 10^{11} photons corresponding to approximately 2×10^4 Gy.

The negligible intensity loss is in agreement with work done by Hamada et al. [11] which presents 10^5 Gy as the critical dose for degradation of the scintillating mechanism, and which furthermore shows that most of the loss in light output is reversible.

The dose reported here is obtained in two 8 h exposures and since the flux was four magnitudes higher compared to typical 3DXRD experiments [12], the longevity of the scintillator is sufficient for years of work. For other applications more radiation resistant materials are used, but this measurement re-establishes the significance of CsI in X-ray imaging.

5. Outlook

The presented sample is the first prototype aiming at high spatial resolution. The promising results imply that the work to develop 1 μm pitched scintillators will continue. Vital aspects in future work will be to obtain a better homogeneity across the scintillator by a better controlled annealing procedure and an increased focus on the surface finishing.

Acknowledgments

The authors are thankful for discussions with and support from N.B. Larsen at RISØ. The authors also gratefully acknowledge support from the Danish National Research Foundation, the Danish Natural Science Research Council (via Dansync) and from the EU's sixth framework program TotalCryst.

References

[1] A. Koch, C. Raven, et al., J. Opt. Soc. Am. A 15 (1998).
[2] M. Di Michiel, J.M. Merino, et al., Rev. Sci. Instrum. 76 (2005).
[3] T. Martin, A. Koch, J. Synchrotron Rad. 13 (2006).
[4] H.F. Poulsen, Crystallogr. Rev. 10 (1) (2004).
[5] C. Piemonte, et al., Nucl. Instr. and Meth. A 541 (1–2) (2005).
[6] H.W. Deckman, et al., J. Vac. Sci. Technol. B 7 (6) (1989).
[7] E. Bigler, F. Polack, Appl. Opt. 24 (7) (1985).
[8] X. Badel, A. Galeckas, et al., Nucl. Instr. and Meth. A 487 (2002).
[9] P. Kleimann, et al., IEEE Trans. Nucl. Sci. NS-47 (1) (2000).
[10] V. Lehmann, Electrochemistry of Silicon, Wiley, New York, 2002.
[11] M.M. Hamada, et al., Nucl. Instr. Phys. Res. A 486 (2002).
[12] S. Schmidt, S.F. Nielsen, et al., Science 305 (2004).